has surpassed the prior world statistics, more live-time will be welcome and allow finer subdivision of the data for cross-checks and estimation of possible mixing parameters.

Still, to claim the atmospheric $\nu$ anomaly is caused by neutrino mixing requires confirmation with as many other signatures as possible. Upward-going muons currently show a mix of results, none obviously refuting or confirming. The upward $\mu$ flux measurement of Super-Kamiokande is consistent with the estimated parameters from the contained vertex sample, but the result is not conclusive. Further analysis of stopping muons and the angular distribution is awaited.

In the end, the best confirmation should come from long-baseline neutrino beams from accelerators. However, according to the preliminary Super-K results, the experiments under construction may have to address lower values of $\Delta m^2$ than when they were conceived.

## 8. Acknowledgements

The author thanks the conference organizers and the participants listed in this paper. He is especially appreciative of his collaborators on Super-Kamiokande for preparing the latest results, which are presented here on their behalf. He gratefully acknowledges financial support by the U.S. Department of Energy.

## REFERENCES

1. T.K. Gaisser *et al.*, Phys. Rev. **D54** (1996) 5578.
2. M. Honda *et al.*, Phys. Lett. **B248** (1990) 193; M. Honda *et al.*, *ibid.***D52** (1995) 4985.
3. G. Barr *et al.*, Phys. Rev. **D39**(1989) 3532; V. Agrawal *et al.*, *ibid.***D53**(1996) 1314; T.K. Gaisser and T. Stanev, Proc. 24th Int. Cosmic Ray Conf.(Rome) Vol.1 (1995) 694.
4. M. Circella *et al.*, Proc. 25th Int. Cosmic Ray Conf.(Durban) Vol.7 (1997) 117.
5. G. Barbiellini *et al.*, Proc. 25th Int. Cosmic Ray Conf.(Durban) Vol.6 (1997) 317.
6. G. Tarlé *et al.*, Proc. 25th Int. Cosmic Ray Conf.(Durban) Vol.6 (1997) 321.
7. T. Stanev, These proceedings.
8. Super-Kamiokande collaboration, To be published.
9. D. Casper *et al.*, Phys. Rev. Lett. **66** (1991) 2561; R. Becker-Szendy, *et al.*, Phys. Rev. **D46** (1992) 3720.
10. K.S. Hirata *et al.*, Phys. Lett. **B205** (1988) 416; K.S. Hirata *et al.*, *ibid.***B280** (1992) 146.
11. W.W.M. Allison *et al.*, Phys. Lett. **B391** (1997) 491
12. T. Kafka, These proceedings.
13. K. Daum *et al.*, Z. Phys. **C66** (1995) 417.
14. M. Aglietta *et al.*, Europhys. Lett. **8** (1989) 611.
15. Y. Fukuda *et al.*, Phys. Lett. **B335** (1994) 237.
16. R. Clark *et al.*, Phys. Rev. Lett. **79** (1997) 345.
17. J. Engel *et al.*, Phys. Rev. **D48** (1993) 3048.
18. K. Inoue, These proceedings.
19. S. Kasuga *et al.*, Phys. Lett. **B374** (1996) 238.
20. J. Flanagan *et al.*, UH-511-880-97, hep-ph/9709438
21. O.G. Ryaznskaya, JETP Lett. **61** (1995) 237.
22. Y. Fukuda *et al.*, Phys. Lett. **B388** (1996) 397.
23. T.K. Gaiser and T. Stanev, BRI-97-28, astro-ph/9708146.
24. T. Montaruli, These proceedings.
25. S. Mikheyev, These proceedings.
26. Y. Totsuka, 28th Int. Symposium on Lepton Photon Interactions, Hamburg, 1997; Kamiokande collaboration, To be published.
27. R. Becker-Szendy *et al.*, Nucl. Phys. **B38** (Proc. Supp.) (1995) 331.
28. P. Lipari and M. Lusignoli, ROME-1190-97, hep-ph/9712278.
29. W. Frati *et al.*, Phys. Rev. **D48** (1993) 1140.
30. P. Lipari *et al.*, Phys. Rev. Lett. **74** (1995) 4384.
31. MACRO collaboration, In preparation.
32. Q.Y. Liu and A.Yu. Smirnov, IC-97-211, hep-ph/9712493.

the usual analytic integration using deep inelastic scattering and parton distribution functions must be handled with care[27,29], especially at low energy[30]. After these considerations, the predicted rate was .14 or .18 depending on the flux model[27]. Based on the agreement of data with prediction, a small excluded region in $\sin^2 2\theta$, $\Delta m^2$ was drawn around $\Delta m^2 = 10^{-3}\mathrm{eV}^2/c^2$, where the strongest deviation would have been found; this happens to be in conflict with the region favored by the Super-K contained vertex data. Super-Kamiokande will also measure the stopping ratio, with the advantage of a very thick detector that stops a large number of upward-going muons; the analysis is in progress.

The second approach uses the shape of the zenith distribution, which may be distorted as the baseline varies from 500 km at the horizon to 12,000 km at the nadir. Because the energy spectrum of the parent neutrinos is broad, $\sim 10-1000$ GeV, the change in shape is gradual, with some steepening at the horizon as the probability decreases for high energy $\nu_\mu$ to oscillate. Figure 5 shows the Super-K measurement of the flux versus zenith angle compared to expectation; recall that the normalization of the prediction is uncertain to $\pm 20\%$. When the normalization of the Monte Carlo is decreased by a factor of $\alpha = 0.83$ to match the data, the $\chi^2$ is 12.7; alternatively, when the normalization is increased by a factor of $\alpha = 1.2$, and $\nu_\mu$ disappearance oscillations are applied with $\sin^2 2\theta = 1$, $\Delta m^2 = .005$, the fit is somewhat better, with a $\chi^2$ of 8.3.

The other experiments listed in Table 5 can make this comparison as well. The scintillator detectors MACRO and Baksan unfortunately have reduced acceptance at the horizontal, so those bins require significant geometric correction. Curiously, even the well-measured upward bins of those two experiments are not smooth and suffer from poor agreement in shape with: (a) no oscillation, (b) any 2-flavor oscillation parameters[7], and (c) each other. Both experimental groups have made extensive checks for a systematic error, but have found no cause[25,31].

[7] A recent preprint considers that matter oscillation with a sterile neutrino crossing the Earth's core may modulate the prediction with features similar to the MACRO data[32].

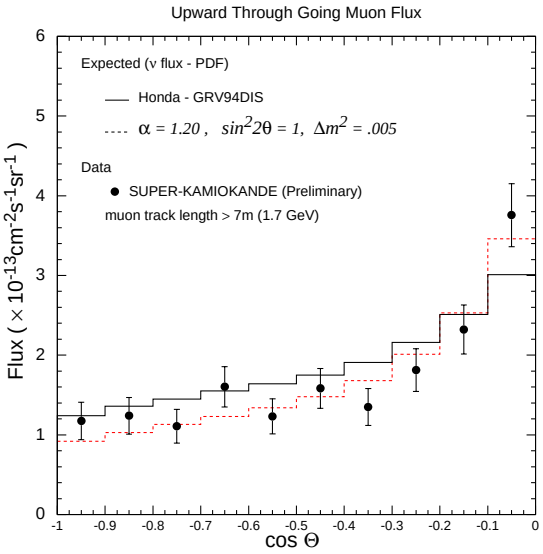


Figure 5. The through-going upward-going $\mu$ flux as a function of zenith angle as measured by Super-Kamiokande. The data points are compared against expectation (solid histogram) and the same expectation with normalization $\alpha = 1.2$ and $\nu$-mixing $\sin^2 2\theta = 1$, $\Delta m^2 = .005$.

## 7. Conclusions

Currently, the evidence for an anomalous ratio of atmospheric neutrino flavors is inconsistent across experiments. Of course, prior results remain intact, and either support or disagree with the anomaly. But the latest results support that a significant discrepancy exists between experiment and prediction. The measurement by Soudan-2 shows that the anomaly is not specific to water Cherenkov detectors. A zenith angle measurement of the Soudan-2 data could be very interesting. Significant new information is taken from the high statistics Super-Kamiokande data: the anomaly is strongly confirmed in $R$ and the zenith angle dependence of $R$. The shape of the zenith angle dependence is very suggestive of neutrino oscillations. The multi-GeV $\mu$-like rate as a function of zenith angle indicates that $\nu_\mu$ disappearance is favored over $\nu_\mu \rightarrow \nu_e$ oscillation. Even though 1.1 years of Super-Kamiokande running

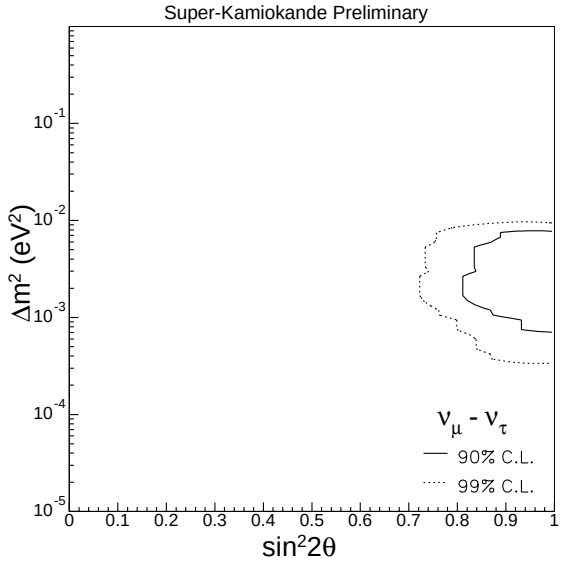


Figure 4. Confidence intervals for $\sin^2 2\theta$ and $\Delta m^2$ based on a $\chi^2$ fit to Super-Kamiokande atmospheric neutrino data binned by lepton identification, lepton momentum and $\cos\Theta$. The solid line is 90% CL, the dashed line is 99% CL.

data, the minimum $\chi^2$ is found to be rather likely, ~30% depending on the details. From the fit, a confidence interval is drawn based on $\chi^2_{min} + 4.6$ (90% CL) such as shown in Fig. 4.

The preferred interval for $\sin^2 2\theta$ is found near 1 because the upward zenith bin with $\langle L \rangle \sim 10,000$ km, presumably has averaged over several oscillation lengths and $P_{\nu\nu'}$ is one half. In a scenario where more than two $\nu$ flavors are mixing, the average value can be less than one half. The $\Delta m^2$ range is determined by the shape of the zenith angle, also considering dependence on $E_\nu$. This 90% confidence interval from Super-Kamiokande prefers a lower range in $\Delta m^2$ than that found by the Kamiokande collaboration[15], which had a minimum $\Delta m^2$ of .005.

## 6. Upward-Going Muons

The above discussion covered neutrino interactions in the fiducial volume of the detector. The other class of atmospheric neutrino event studied is that of $\nu_\mu$ interactions in the rock around the detector, where the final state muon enters the sensitive region of the detector. To separate these from ordinary cosmic ray muons, the muon must be upward-going, or come from the direction of a known thick overburden. The parent neutrino energy is 10–1000 GeV, significantly higher than for contained events.

There are several current measurements of the total rate of upward-going muons. In addition to the water Cherenkov detectors described elsewhere in this paper, MACRO and Baksan are large area scintillator detectors that distinguish upward-going muons by time-of-flight; T. Montaruli (MACRO) and S. Mikheyev (Baksan) have presented updated results at this conference. The measured and expected event rates are compared in Table 5; the experiments are listed in order of increasing absorber depth for directly vertical muons. The uncertainty in the measured number of events is statistical only; some experiments have estimated that the uncertainty due to experimental systematics could be as large as 8%. The uncertainty in the expected number of events is a common 15–20%, due mostly to the uncertainty in the absolute flux. Considering this, in no case is a significant deficit of muons measured, but the measurements are generally low compared to expectation.

Table 5
Summary of through-going upward-$\mu$ totals.

| | Number of Events | |
|---|---|---|
| Experiment | Measured | Expected |
| MACRO[24] | $350 \pm 19$ | 472 |
| Baksan[25] | $558 \pm 24$ | 557 |
| Kamiokande[26] | $373 \pm 19$ | 414 |
| IMB[27] | $539 \pm 23$ | 550 or 625 |
| Super-K[8] | $410 \pm 20$ | 445 |

There are two other approaches that probe neutrino oscillations[28] using upward-going muons. IMB measured the ratio of stopping upward muons ($\langle E_\nu \rangle \sim 10$ GeV) to through-going upward muons ($\langle E_\nu \rangle \sim 100$ GeV) to be $0.16 \pm .02$. Although much of the flux uncertainty cancels out,

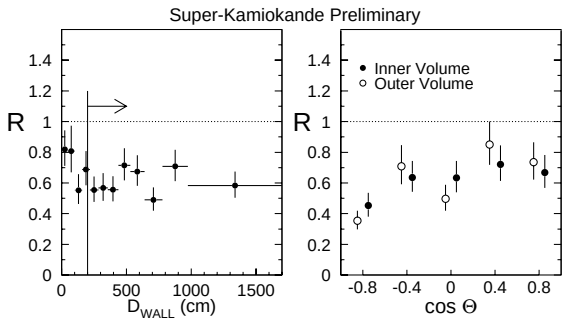


Figure 2. (A) $R$ for the sub-GeV samples as a function of distance from the PMT wall ($D_{WALL}$). (B) $R$ versus zenith angle for two concentric fiducial volumes: $5 > D_{WALL} > 2$ meters (outer) and $D_{WALL} > 5$ meters (inner).

from below ($\cos\Theta < 0$).

The significance of this result can be easily evaluated by calculating the up-down asymmetry $A = (N_{down} - N_{up})/(N_{down} + N_{up})$ where up and down are defined by $\cos\Theta < -.2$ and $> .2$ respectively (Tab.4). Besides other interesting possibilities[20], the distribution of $A$ is nicely described by a gaussian variance. For multi-GeV events, $N_{up}$ and $N_{down}$ should be nearly symmetrical, whereas $A$ for $\mu$-like data (FC+PC) differs from expectation by greater than $5\sigma$.

Table 4
Up-down asymmetry for multi-GeV data.

| Sample | $N_{up}$ | $N_{down}$ | $A$ |
|---|---|---|---|
| $\mu$-like data | 102 | 195 | 0.313±0.055 |
| $e$-like data | 76 | 90 | 0.084±0.077 |
| $\mu$-like MC | 1669 | 1707 | 0.013±0.017 |
| $e$-like MC | 596 | 589 | -0.006±0.029 |

The dashed line in Fig.3 represents an oscillation hypothesis[6] of ($\sin^2 2\theta = 1, \Delta m^2 = .005$) for $\nu_\mu$ disappearance. The overall normalization is adjusted upward (thus the $e$-like rate increases

[6] The values (1, .005) represent a test point; the exact best fit location can change when the technique or data sample changes since the minimum is fairly flat.

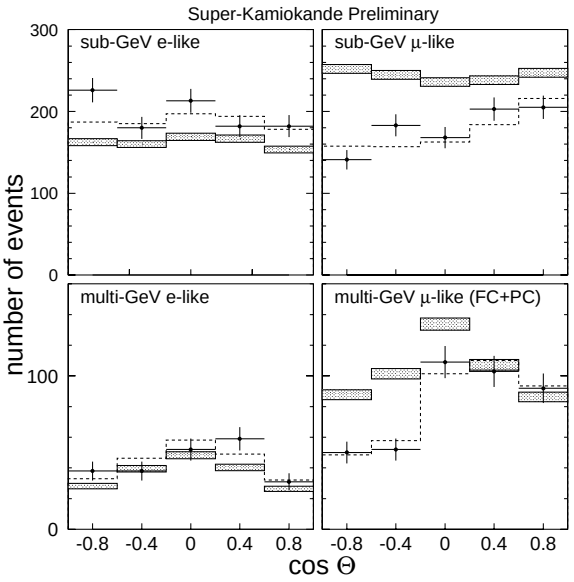


Figure 3. The number of $\mu$-like and $e$-like events as a function of zenith angle. The solid histograms are the Monte Carlo expectation with no neutrino oscillation; the thickness represents the statistical uncertainty in the Monte Carlo sample. The dashed line shows the expected shape for $\nu_\mu \rightarrow \nu_\tau$ oscillation with $\sin^2 2\theta = 1$ and $\Delta m^2 = .005\mathrm{eV}^2/c^2$.

to better match the data, even when $\nu_e$ mixing is not considered) while (2) is used to calculate the probability of $\nu_\mu$ disappearance and reweight the Monte Carlo. The $\nu$ travel distance $L$ is calculated as a function of energy and flavor based on a production height model[23]. The oscillation hypothesis provides a reasonable fit to the data, certainly better than the null hypothesis.

The exact details of fitting the data to estimate possible mixing parameters are still being evaluated. Using a method similar to that used by Kamiokande[15], $\chi^2$ terms are formed between the data and Monte Carlo prediction [modified by $P_{\nu\nu'}(\sin^2 2\theta, \Delta m^2)$], binned in zenith angle, energy, and flavor (values of $R$ are not used directly in the fit). The normalization, $N_\mu/N_e$ ratio and systematic terms are allowed to adjust and contribute to the $\chi^2$. For the Super-Kamiokande

the difference in value from the first analysis is understood to be due to differences in analysis methods and within their systematic uncertainties. In sum, the independent analysis provides reassurance that the deviation of $R$ from unity is not due to experimental mistakes.

To consider that the anomalous $R$ is due to neutrino oscillation, one looks for a path length or energy dependence of the effect. The probability of two-flavor neutrino oscillation from $\nu$ to $\nu'$ is given by:

$$P_{\nu\nu'} = \sin^2 2\theta \sin^2 1.27 \frac{\Delta m^2(\mathrm{eV}^2/c^2) L(\mathrm{km})}{E(\mathrm{GeV})}, \quad (2)$$

where $\theta$ and $\Delta m^2 \equiv |m_\nu^2 - m_{\nu'}^2|$ are fundamental parameters that govern the neutrino mixing, and $L$ and $E$ are the path length and energy of the neutrino. The final state lepton direction and energy are correlated with the incoming neutrino; for the sub-GeV sample, the mean opening angle for $\nu_\mu$–$\mu$ is 54°, for $\nu_e$–$e$ it is 62°; for the multi-GeV sample it improves to $< 15°$.

The samples are divided into 5 $\cos\Theta$ bins where $\Theta$ is the angle between the outgoing lepton direction and the nadir[5]; so down-going neutrinos that are produced directly overhead, with short travel distance, populate the bin near $\cos\Theta = 1$. Calculating $R$ for each zenith bin results in Fig. 1. A slight asymmetry is evident in the sub-GeV sample, and a strong asymmetry is evident in the multi-GeV sample. If there were no anomaly, the $R$ values would be around 1; for hypothetical oscillation parameters of $\sin^2 2\theta = 1$ and $\Delta m^2 = .005$ eV$^2$/c$^2$, the dashed line is expected, and is a better match to the data.

It is interesting to check the result as a function of position in the detector because (a) some reconstruction algorithms are less certain for vertices close to the PMT wall, and (b) possible backgrounds, such as neutrons from nearby cosmic rays [21,22], or entering events that evade the outer detector veto, would accumulate near the fiducial boundary. Figure 2a shows $R$ versus distance from the PMT wall, where the fiducial volume is found at 2 meters. Figure 2b shows the zenith angle dependence of R, dividing the data into two approximately equal fiducial volumes: an outer volume between 2–5 m from the PMT wall and an inner volume greater than 5 m from the wall. There is no variation of the result due to the fiducial boundary evident in either figure.

[5]Caveat: the IMB collaboration used the opposite definition, so down-going neutrinos are near $\cos\Theta = -1$ in their publications.

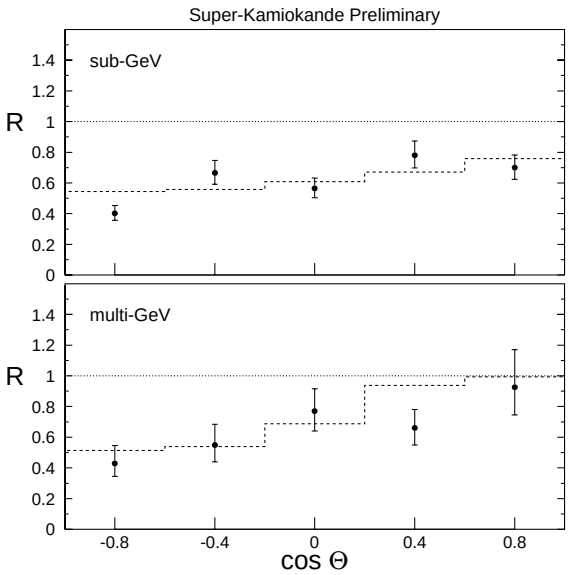


Figure 1. The zenith angle dependence of $R$ for sub-GeV and multi-GeV atmospheric neutrino samples from Super-Kamiokande. The dashed line shows the expected shape for $\nu_\mu \to \nu_\tau$ oscillation with $\sin^2 2\theta = 1$ and $\Delta m^2 = .005$ eV$^2$/c$^2$.

The double-ratio of $(\mu/e)_{DATA}$ to $(\mu/e)_{MC}$ is useful to illustrate the effect, but it does not indicate whether $\mu$ or $e$ rates (or both) are affected. Furthermore, $R$ is not so practical for statistical tests. Figure 3 shows the $\mu$ and $e$ rates separately for sub-GeV and multi-GeV (FC+PC) compared to Monte Carlo prediction. The solid bands are the absolute prediction, where the height of the band is equal to the Monte Carlo statistical uncertainty. Not shown is the ±20% normalization uncertainty, which is highly correlated bin-to-bin, between $\mu$ and $e$, and between sub-GeV and multi-GeV. Even accounting for this uncertainty, it is apparent that the anomalous $R$ is dominated by a deficit of $\mu$-like events coming

Table 2
Event summary for 25.5 kt·year sample of fully-contained atmospheric neutrinos in Super-Kamiokande. Monte Carlo breakdown uses Honda flux.

| | | Monte Carlo prediction | | Monte Carlo breakdown | | |
|---|---|---|---|---|---|---|
| | Data | Bartol[3] | Honda[2] | CC-$\nu_\mu$ | CC-$\nu_e$ | NC |
| sub-GeV $e$-like | 983 | 788.9 | 812.2 | 2% | 88% | 10% |
| sub-GeV $\mu$-like | 900 | 1185.4 | 1218.3 | 96% | 0.5% | 4% |
| sub-GeV multi-ring | 696 | 753.7 | 759.2 | 43% | 24% | 33% |
| multi-GeV $e$-like | 218 | 190.9 | 182.7 | 7% | 84% | 9% |
| multi-GeV F.C. $\mu$-like | 176 | 229.7 | 229.0 | 99% | 0.5% | 0.4% |
| multi-GeV P.C. ($\mu$-like) | 230 | 305.0 | 287.7 | 98% | 1.5% | 0.6% |
| multi-GeV multi-ring | 398 | 450.1 | 433.6 | 55% | 30% | 15% |

$$\text{multi-GeV}\begin{cases} 0.659^{+0.058}_{-0.053}\pm 0.081 & \text{(Honda flux)} \\ 0.665^{+0.059}_{-0.053}\pm 0.082 & \text{(Bartol flux).} \end{cases}$$

For both the high and low energy samples there is a significant deviation of the $\mu/e$ ratio from the expected value of 1. The leading contributions to the systematic uncertainty in $R$ are: $(\nu_\mu/\nu_e)$ flux (5%), neutrino cross section (4.6% for sub-GeV and 5.8% for multi-GeV), and single-ring selection (3% for sub-GeV and 6% for multi-GeV).

It is informative to check the relative rate of $\mu$-decay associated with the event sample. The decay electrons are detected as time separated hits from the neutrino interaction; most come either from associated $\pi^+ \to \mu^+ \to e^+$, or directly from $\mu^\pm \to e^\pm$ in CC-$\nu_\mu$ interactions. The performance of $e/\mu$ identification algorithms is no longer in question [19], but the measured $\mu$-decay fractions check that the associated pion production is reasonably modeled in the Monte Carlo. Table 3 shows that the expected fraction of $\mu$-decay agrees well with the prediction; the fraction of $\mu$-decay found in stopping cosmic ray muons verifies the efficiency of the reconstruction.

Table 3
$\mu$-decay fractions.

| Percentage of events with $\geq 1$ $\mu$-decay | | |
|---|---|---|
| | Data | Monte Carlo |
| stopping CR $\mu$ | $74.0 \pm 0.3\%$ | $72.9 \pm 0.4\%$ |
| $\mu$-like | $67.6 \pm 1.6\%$ | $68.1 \pm 0.1\%$ |
| $e$-like | $9.3 \pm 0.9\%$ | $8.7 \pm 0.3\%$ |
| Percentage of events with $\geq 2$ $\mu$-decay | | |
| | Data | M.C. |
| stopping CR $\mu$ | $0.0 \pm 0.0\%$ | $0.0 \pm 0.0\%$ |
| $\mu$-like | $2.9 \pm 0.6\%$ | $4.1 \pm 0.1\%$ |
| $e$-like | $0.2 \pm 0.1\%$ | $0.1 \pm 0.0\%$ |

The Super-Kamiokande group had two independent analysis efforts that were used to check each other and minimize the possibility that some mistake would be made. The data were separated after electronics calibration of the PMT data to photoelectrons and nanoseconds. Otherwise, everything was coded independently, including event reduction and reconstruction, Monte Carlo generation, and estimation of the energy scale. Beyond the independent code, the major differences in the second analysis were: (a) data reduction involved no scanning, (b) single-ring selection was based on an algorithm that classified events as single-ring or multiple-ring without attempting to count the number of rings, (c) $e/\mu$ identification was somewhat simpler and less efficient (97% vs >99%), (d) some details of vertex and direction reconstruction were different.

Upon comparison, the independent analyses were in exceptional agreement. Of the sub-GeV events found in the fiducial volume by the second analysis, 99.9% were found in the data sample of the first analysis, with 89% in the fiducial volume, consistent with the vertex fit resolution. Single-ring classification was in agreement 90% of the time. Comparing common events in the fiducial single-ring sub-GeV sample, vertices agreed to 84 cm RMS, direction agreed to 2.5°, momentum agreed to 0.5%, 97% of the events agreed in particle identification. The value of $R$ for the sub-GeV sample of the second analysis is: $0.65 \pm 0.03 \pm 0.05$;

to $\nu_e$ cross sections[17], it interesting that the anomaly has also been seen in Fe as well as in $H_2O$. What the difference is between these results and those of Fréjus and NUSEX (beyond what may be encompassed by large uncertainties) remains to be explained.

## 5. Super-Kamiokande

Super-Kamiokande is the next generation water Cherenkov experiment after IMB and Kamiokande. The detector resides nearby the old Kamiokande detector in a mine near Kamioka, Japan. However, it is much larger (22.5 kton fiducial mass, versus 1 kton for Kamiokande and 3.3 kton for IMB). It is instrumented with 22,000 PMTs, each 50 cm across, such that 40% of the inner surface area is active photocathode. The PMTs and electronics are of advanced design, with 2.5 ns RMS timing for single photoelectrons. The inner detector is surrounded by an outer volume of water ~2.7 m thick that shields against incoming radioactivy and is instrumented with PMTs to tag penetrating muons. Further description of the detector, as well as new measurements of the $^8B$ solar neutrino flux were presented at this conference by K. Inoue[18].

The measurement from Super-Kamiokande is the result of a 414.2 live-day exposure (25.5 kton·yrs) during the period from May 1996 to October 1997. The data is reduced from approximately 800K events per day to about 30 events per day by a series of software cuts. The most powerful requirement is the absence of hits in the outer detector, which indicates a fully contained (FC) interaction. The remaining events are then filtered by a visual scan, where the principal backgrounds are: (1) cosmic ray muons that evade the outer detector veto, typically by entering along cable bundles and then stopping in the detector, and (2) "flashing" PMTs that emit light due to internal corona discharge. The partially contained sample is formed by a different reduction program from the same exposure[4], since outer detector hits are now expected, and the background rejection of entering cosmic rays is different. A 10.0 live-year Monte Carlo sample of $\nu$ interactions is passed through the same reduction chains, except for the visual scan.

The remaining events, both data and Monte Carlo, are passed through the same reconstruction code to: (a) fit the vertex of the interaction, by residual PMT timing, (b) count the number of Cherenkov rings, (c) estimate the direction of each ring, (d) estimate the energy of each ring, (e) determine the particle type ($\mu$-like,$e$-like) for each ring, and (f) count the number of $\mu$-decay electrons that follow each event. Most of the analysis is then done with the sample of events in which the number of rings found in (b) is exactly one. In most cases, this is the final state lepton from a charged current neutrino interaction; the principal contamination is single pion production associated with neutral current (NC) interactions.

The absolute energy scale was determined to $\sim 2.5\%$ accuracy using several calibration signatures: LINAC electrons, radioactive sources, $\pi^0$s and cosmic ray muons. About 9 photoelectrons are recorded for 1 MeV of visible energy. Conversion to lepton momentum takes into account the Cherenkov cutoff for muons.

Data samples are defined using the same kinematic criteria as in the Kamiokande experiment: $p_e > 100$ MeV/c, $p_\mu > 200$ MeV/c, and $E_{vis} \leq 1.33$ GeV for sub-GeV; $E_{vis} > 1.33$ GeV for multi-GeV FC. The partially contained sample is specified by a vertex in the inner detector and correlated hits in the outer detector; the minimum visible energy required is $\sim 350$ MeV. Because $\langle E_\nu \rangle$ is >> 1 GeV for the PC sample, these data are added to to the FC multi-GeV sample; the CC lepton is assumed to be a muon, and no single-ring is required. The fiducial sample is restricted to events with vertex 2 m from the PMT wall (22.5 kton).

The event totals are listed in Table 2 along with the totals for the Monte Carlo samples, scaled to 25.5 kton·yrs. These yield the following values of $R = (N_\mu/N_e)_{DATA}/(N_\mu/N_e)_{MC}$:

$$\text{sub-GeV} \begin{cases} 0.610^{+0.029}_{-0.028} \pm 0.049 & \text{(Honda flux)} \\ 0.609^{+0.029}_{-0.028} \pm 0.049 & \text{(Bartol flux)} \end{cases}$$

[4] The results quoted here are updated from previous conference presentations, where PC livetime was somewhat less than FC livetime, and PC data was scaled (by ~ 1.1) when FC+PC results were plotted.

where $N$ refers to the number of events where the final state lepton is classified as $\mu$-like or $e$-like by some identification algorithm. As mentioned above, the ratio of $\nu_\mu$ to $\nu_e$ flux is accurately predicted; in addition, other theoretical and experimental uncertainties largely cancel. Table 1 lists previous measurements[2] of $R$ for $E_\nu \sim 1$ GeV, including the new results from Soudan and Super-Kamiokande discussed in this paper. The kinematic limits differ somewhat from experiment to experiment, with minimum lepton momenta requirements from 100 to 200 MeV/c. Kamiokande restricted their sample to[3] $E_{vis} < 1.33$ GeV, IMB to $p < 1.5$ GeV; the other experiments did not specify an upper limit, but all results are dominated by $\sim 1$ GeV neutrinos.

Table 1
Summary of $R$ measurements, $E_\nu \sim 1$ GeV.

| Experiment | kt-yr | events | R (data/MC) |
|---|---|---|---|
| Super-K[8] | 25.5 | 1853 | $0.61 \pm .03 \pm .05$ |
| IMB[9] | 7.7 | 610 | $0.54 \pm .05 \pm .11$ |
| Kam.[10] | 7.7 | 482 | $0.60^{+.06}_{-.05} \pm .05$ |
| Soudan-2[12] | 3.2 | ~200 | $0.61 \pm .15 \pm .05$ |
| Fréjus[13] | 2.0 | 200 | $1.00 \pm .15 \pm .08$ |
| NUSEX[14] | 0.7 | 50 | $0.96^{+.32}_{-.28}$ |

Kamiokande also studied events with $E_{vis} > 1.33$ GeV (multi-GeV) and included partially contained (PC) events where a track was detected exiting the inner detector[15]. They measured a low value for $R$ of $0.57^{+0.08}_{-0.07} \pm 0.07$, but more interesting was the dependence of $R$ on zenith angle. Neutrinos that travelled $\sim 10^4$ km from below showed a small value of $R$, but those that travelled $\sim 10$ km from above agreed with expectation, suggesting an oscillation length somewhere in between.

[2] The first uncertainty quoted is statistical, the second is systematic; this convention will be used throughout the paper.
[3] Visible energy ($E_{vis}$) is defined as the energy of an electromagnetic shower that produces a given amount of Cherenkov light.

Most of the IMB multi-GeV exposure had a restriction on the maximum number of PMT hits (to concentrate on proton decay); the restriction was eventually removed, so they made a separate analysis[16] of their last 2.1 kt·years for $E_{vis} > .95$ GeV and measured $R = 1.40^{+0.45}_{-0.34} \pm 0.14$ with no zenith dependence. The caveats are: limited statistics of 72 events (some overlapping with Ref.[9]); no outer detector to help identify PC muons; coarser sampling (4% photon coverage), resulting in only 90% correct $e/\mu$ identification.

## 4. Soudan-2

Until recently, atmospheric neutrino results seemed to be divided between water Cherenkov detectors [9,10] (anomalous) and iron calorimeters [13,14] (as expected). The Soudan-2 collaboration, which operates a fine-grained iron tracking calorimeter in Minnesota, U.S.A., has recently published results [11] which support the anomaly seen in the water Cherenkov experiments.

At this meeting, T. Kafka has updated the results from Soudan-2 to 3.2 kt·years[12]. They measure 91 single-prong track events (mostly charged current (CC) $\nu_\mu$) with $p > 100$ MeV/c, and 137 shower events (mostly CC-$\nu_e$) with $p > 150$ MeV/c. The interaction vertex is allowed as close as 20 cm from the edge of the detector; with only 32 gm/cm$^2$ of shielding they observe a significant (25-30%) background from gamma rays and neutrons associated with nearby cosmic rays. However, they use an active shield of proportional tube planes lining the detector hall to veto most nearby cosmic rays, as well as separately estimate the remaining background rate as a function of flavor, depth into the detector, and energy.

After background subtraction, the number of shower events matches their Monte Carlo prediction; however they observe 37% fewer tracks than they predict. Since the total flux is uncertain, it is better to consider the double-ratio, which they measure to be $R = 0.61 \pm 0.15 \pm 0.05$. Regarding the atmospheric neutrino anomaly, this is a considerable new piece of information, as the systematics are very different from the water Cherenkov detectors. Although there are no demonstrated nuclear effects that would change the ratio of $\nu_\mu$

# Experimental Measurements of Atmospheric Neutrinos

Edward Kearns[a]

[a]Department of Physics, Boston University
590 Commonwealth Ave.
Boston, MA 02215

This talk reports the latest indications of an anomaly in the measurements of atmospheric neutrinos. New results from Soudan-2 and Super-Kamiokande provide evidence that the ratio of $\nu_\mu$ to $\nu_e$ interactions is not as expected. High energy Super-Kamiokande data indicates the cause is a deficit of upward-going $\nu_\mu$, and the zenith angle dependence of the effect is consistent with neutrino oscillations. Upward-going muon measurements by several detectors are discussed, but in total they provide inconclusive evidence for the anomaly.

## 1. Introduction

Large underground detectors originally built to search for proton decay are also exposed to a flux of neutrinos created by cosmic ray showers in the upper atmosphere. Neutrino interactions in the detector can mimic proton decay, and therefore a great effort has gone into predicting the rate and topology of the neutrino background. A byproduct of this effort has been the recognition of an anomaly: the relative rate of $\nu_\mu$ and $\nu_e$ interactions disagrees with expectation, and the baseline and energy dependence of the disagreement suggests that neutrino oscillation may be the culprit.

The nature of these experiments is to measure the rate of neutrino interactions in the detector and to compare that rate with theoretical prediction. The theoretical task is to predict the neutrino flux as a function of energy, direction, and flavor, taking into account measurements of cosmic ray flux, geomagnetic cutoff, and production and decay of secondary mesons. Detailed Monte Carlo programs are used to estimate the cross section for neutrino interaction and simulate the response of the detector. The experimental task is to measure as much as possible about the neutrino interaction, in particular, the energy, direction, and flavor of the final state lepton, from which the neutrino properties are inferred.

## 2. Flux prediction

One of the tenets of the atmospheric neutrino anomaly is that the flux ratio[1] $(\nu_\mu/\nu_e)$ is more accurately predicted that the $\nu_\mu$ or $\nu_e$ flux alone. The principal effect is that cosmic ray showers consist mostly of pions, which decay to $\mu + \nu_\mu$, and the $\mu$ decays to to $e + \nu_e + \nu_\mu$, resulting in a flux ratio $(\nu_\mu/\nu_e) \sim 2$. The authors of detailed calculations of the flux models have collaborated to compare results[1] and reached an understanding of many of the differences between their earlier publications. Two updated calculations[2,3] cover a wide energy range (10 MeV–10 TeV) and are used by current experiments. There are now also an assortment of new high altitude $\mu$ measurements available for comparison [4–6]. Further details of flux calculations were presented at this meeting by T. Stanev[7]. However, there is currently no indication that poor knowledge of the predicted flux could be responsible for the experimental anomalies described below.

## 3. Summary of results

To study the $(\nu_\mu/\nu_e)$ flux ratio, most experiments calculate the double-ratio or ratio-of-ratios:

$$R = \frac{(N_\mu/N_e)_{DATA}}{(N_\mu/N_e)_{MC}}, \qquad (1)$$

[1] technically $(\nu_\mu + \bar{\nu}_\mu)/(\nu_e + \bar{\nu}_e)$